

Rapidity and system size dependence of anisotropic flows in relativistic heavy ion collisions

Che Ming Ko^{a*}, Lie-Wen Chen^{b†}

^aCyclotron Institute and Physics Department,
Texas A&M University, College Station, Texas 77843-3366, USA

^bInstitute of Theoretical Physics,
Shanghai Jiao Tong University, Shanghai 200240, China

We report results from a multiphase transport (AMPT) model on the rapidity and system size dependence of charged hadron anisotropic flows in nuclear collisions at the Relativistic Heavy Ion Collider (RHIC).

1. Introduction

The azimuthal anisotropy of hadron transverse momentum distributions in heavy ion collisions at RHIC is sensitive to the properties of produced matter. In the framework of transport approach, it was shown in Ref.[1] using the ZPC model [2] that the value of the second harmonic, i.e., the elliptic flow, depends sensitively on the magnitude of parton scattering cross sections. With a more realistic collision dynamics via the AMPT model [3,4], it was further shown that the observed large elliptic flow and its ordering according to hadron masses [5] as well as high-order anisotropic flows [6] could be explained if partons scatter with cross sections much larger than those given by the perturbative QCD. Including also charm quarks in the AMPT model [7], the observed large elliptic flow of electrons from the decay of charmed mesons is again consistent with a large charm scattering cross section. In the present contribution, recent results from the AMPT model on the rapidity and collision system dependence of anisotropic flows are presented [8–10].

2. The AMPT model

The AMPT model is a hybrid model that uses minijet partons from hard processes and strings from soft processes in the HIJING model [11] as the initial conditions for modelling heavy ion collisions at ultra-relativistic energies. In the default version, time evolution of resulting minijet partons is described by the ZPC model [2] with an in-medium cross section derived from the lowest-order Born diagram with an effective gluon screening mass taken as a parameter for fixing the magnitude and angular distribution of parton scattering

*Work supported by US National Science Foundation under Grant No. PHY-0457265 and the Welch Foundation under Grant No. A-1358.

†Work supported by National Natural Science Foundation of China under Grant Nos. 10105008 and 10575071.

cross section. After minijet partons stop interacting, they are combined with their parent strings, as in the HIJING model with jet quenching, to fragment into hadrons using the Lund string fragmentation model as implemented in the PYTHIA program [12]. The final-state hadronic scatterings are then modelled by the ART model [13]. In an extended string melting version of the AMPT model [5], hadrons that would have been produced from string fragmentation are converted to valence quarks and/or antiquarks in order to model the initially formed partonic matter. Interactions among these partons are again described by the ZPC parton cascade model. The transition from the partonic matter to the hadronic matter is achieved using a simple coalescence model, which combines two nearest quark and antiquark into mesons and three nearest quarks or antiquarks into baryons or anti-baryons that are close to the invariant mass of these partons.

3. Pseudorapidity dependence of anisotropic flows

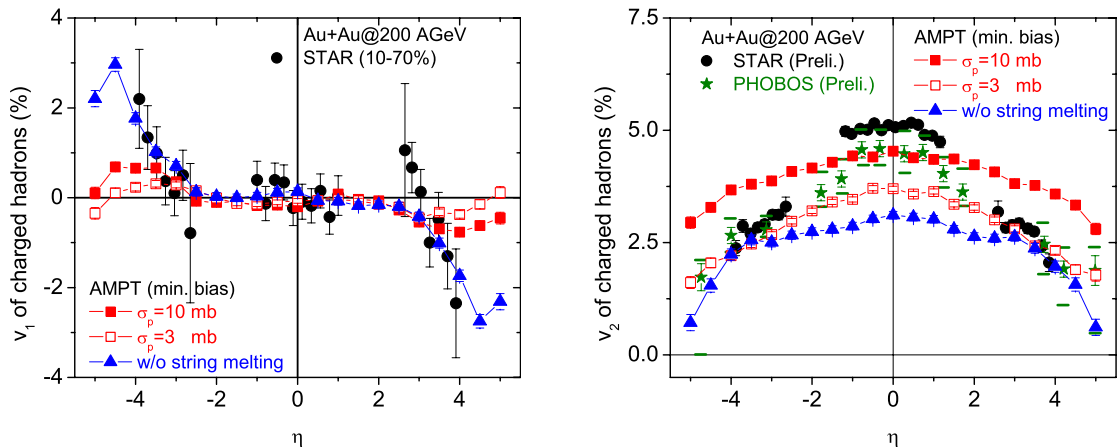


Figure 1. Pseudorapidity dependence of v_1 (left panel) and v_2 (right panel) in minimum bias events of Au + Au collisions at $\sqrt{s} = 200$ AGeV.

Results from the AMPT model on the pseudorapidity (η) dependence of the directed (v_1) and elliptic (v_2) flows of charged hadrons in minimum bias events of Au + Au collisions at $\sqrt{s} = 200$ AGeV are shown, respectively, in the left and right panels of Fig. 1 [8]. For v_1 , both the default version and the version with string melting can reproduce approximately the STAR data (solid circles) [14] around the mid-pseudorapidity region, while only the default version can describe the data at large $|\eta|$. For v_2 , the string melting scenario with a parton scattering cross section of $\sigma_p = 10$ mb (solid squares) describes very well the PHOBOS data (solid stars) [15] around mid- η ($|\eta| \leq 1.5$) but a smaller $\sigma_p = 3$ mb (open squares) or the default version (solid triangles) gives a better description of both PHOBOS and STAR [16] data at large pseudorapidity ($|\eta| \geq 3$). These interesting features imply that initially the matter produced at large pseudorapidity is dominated by strings while that produced around mid-rapidity mainly consists of partons. This is a reasonable picture as particles at large rapidity are produced later in time when the volume of the system is large and the energy density is small.

4. System size dependence of anisotropic flows

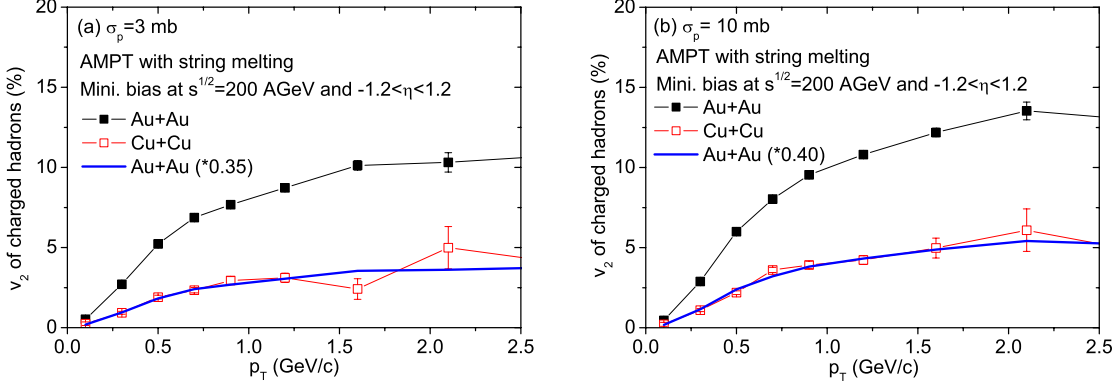


Figure 2. Transverse momentum dependence of the v_2 of mid-rapidity charged hadrons in minimum bias events of Au+Au (solid squares) and Cu+Cu (open squares) collisions at $\sqrt{s} = 200$ AGeV.

In Fig.2, results from the AMPT model with string melting for charged hadron elliptic flows in minimum bias Cu+Cu and Au+Au collisions at $\sqrt{s} = 200$ AGeV are shown for parton scattering cross sections of $\sigma_p = 3$ mb (left panel) and 10 mb (right panel) [9]. It is seen that the elliptic flow in the lighter Cu+Cu collisions is about a factor of 3 smaller than that in the heavier Au+Au collisions at same energy as shown by solid lines. This is consistent with the linear scaling of the system size as well as the combined effect of the initial energy density and spatial eccentricity.

5. Anisotropic flows in collisions of asymmetric systems

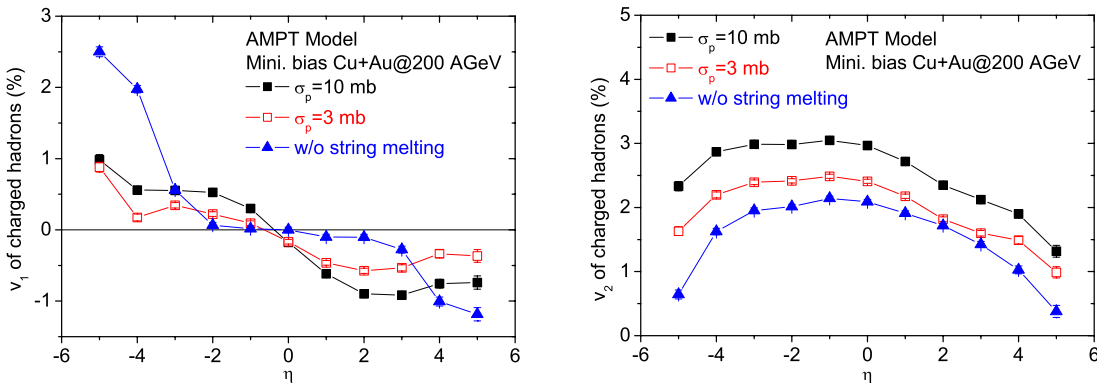


Figure 3. Pseudorapidity dependence of v_1 (left panel) and v_2 (right panel) for charged hadrons in minimum bias events of Cu+Au collisions at $\sqrt{s} = 200$ AGeV.

In Fig.3, the pseudorapidity dependence of v_1 (left panel) and v_2 (right panel) for

charged hadrons in minimum bias events of Cu+Au collisions at $\sqrt{s} = 200$ AGeV are shown for the string melting scenario with parton scattering cross sections $\sigma_p = 3$ (open squares) and 10 mb (solid squares) as well as the default AMPT model without string melting (solid triangles) [10]. Comparing with results in symmetric Au+Au collisions, we find that charged hadrons produced around mid-rapidity in asymmetric Cu+Au collisions display a stronger v_1 and their v_2 is also more sensitive to the parton cross section used in the parton cascade. Furthermore, both v_1 and v_2 are appreciable and show an asymmetry in the forward and backward rapidities.

6. Summary

Using the AMPT model, we have studied the rapidity and colliding system size dependence of anisotropic flows in heavy ion collisions at RHIC. We find that results on the rapidity dependence of anisotropic flows suggest that a partonic matter is formed during early stage of relativistic heavy ion collisions only around mid-rapidity and that strings remain dominant at large rapidities. Furthermore, to reproduce the experimental data requires a parton cross section that is larger than that given by the perturbative QCD, indicating that nonperturbative effects are important in the produced partonic matter at RHIC. Also, a linear scaling with the colliding system size is observed for the elliptic flow of charged hadrons in minimum bias collisions. For collisions of asymmetric systems, there is a strong v_1 around mid-rapidity, and both v_1 and v_2 are asymmetric in the forward and backward rapidities. Experimental verification of latter predictions will be very useful in testing the AMPT model as well as in understanding the dynamics of the partonic matter produced in the collisions.

REFERENCES

1. B. Zhang, M. Gyulassy, and C. M. Ko, Phys. Lett. B 455 (1999) 45.
2. B. Zhang, Comput. Phys. Commun. 109 (1998) 193.
3. B. Zhang, C. M. Ko, B. A. Li, and Z. W. Lin, Phys. Rev. C 61 (2000) 067901.
4. Z. W. Lin, S. Pal, C. M. Ko, B. A. Li, and B. Zhang, Phys. Rev. C 64 (2001) 011902 ; Nucl. Phys. A 698 (2002) 375; nucl-th/0411110.
5. Z. W. Lin and C. M. Ko, Phys. Rev. C 65 (2002) 034904.
6. L. W. Chen, C. M. Ko, and Z. W. Lin, Phys. Rev. C 69 (2004) 031901(R).
7. B. Zhang, L. W. Chen, and C. M. Ko, Phys. Rev. C 72 (2005) 024906.
8. L. W. Chen, V. Greco, C. M. Ko, and P. Kolb, Phys. Lett. B 605 (2005) 95.
9. L. W. Chen and C. M. Ko, nucl-th/0505044.
10. L. W. Chen and C. M. Ko, nucl-th/0507067.
11. X. N. Wang and M. Gyulassy, Phys. Rev. D 44 (1991) 3501.
12. T. Sjostrand, Comput. Phys. Commun. 82 (1994) 74.
13. B. A. Li and C. M. Ko, Phys. Rev. C 52 (1995)2037; B. A. Li, A. T. Sustich, B. Zhang, and C.M. Ko, Int. Jour. Phys. E 10 (2001) 267.
14. J. Adams *et al.* [STAR Collaboration], Phys. Rev. Lett. 92 (2004) 062301.
15. S. Manly for the PHOBOS Collaboration, Nucl. Phys. A 715 (2003) 611c.
16. M. D. Oldenburg for the STAR Collaboration, 2004, nucl-ex/0403007.